

**LASER INTERFEROMETER GRAVITATIONAL WAVE OBSERVATORY
-LIGO-
CALIFORNIA INSTITUTE OF TECHNOLOGY
MASSACHUSETTS INSTITUTE OF TECHNOLOGY**

Technical Note	LIGO-T04XXXX-00-R	24/05/04
Sidebands of Sidebands in the 40m System		
B.W. Barr and O. Miyakawa		

Distribution of this draft:
Detector

This is an internal working note
of the LIGO Project.

California Institute of Technology	Massachusetts Institute of Technology
LIGO Project - MS 18-34	LIGO Project - MS 20B-145
Pasadena, CA 91125	Cambridge, MA 01239
Phone (626) 395-2129	Phone (617) 253-4824
Fax (626) 304-9834	Fax (617) 253-7014
E-mail: info@ligo.caltech.edu	E-mail: info@ligo.mit.edu

WWW:<http://www.ligo.caltech.edu/>

1 Introduction

The Caltech 40 m Detuned Resonant Sideband Extraction (DRSE) interferometer is the final stage of development for length sensing and control for Advanced LIGO. To this end an RF (radio frequency) sensing scheme was developed utilising two sets of phase sidebands at $f_1 = \pm 33$ MHz and $f_2 = \pm 166$ MHz. A detailed discussion of this scheme can be found in the LIGO internal documents LIGO-T010115-00-R (conceptual design) and LIGO-T040081-00-R (lock acquisition scenario).

The sensing scheme breaks the interferometer into five lengths (or Degrees Of Freedom (DOFs)) to be controlled: common mode arm motion L_+ detected at the symmetric port (SP) by demodulating at f_1 , differential mode arm motion L_- detected at the antisymmetric port (AP) by demodulating at f_2 , power recycling cavity (PRC) motion l_+ detected at SP using the beat between f_1 and f_2 , Michelson motion l_- detected at AP using the beat between f_1 and f_2 and signal recycling cavity (SRC) motion l_s detected using light picked off from within the PRC/SRC cavity (PO) at the beat between f_1 and f_2 .

Key to this discussion is the fact that the inner DOFs in this scenario (l_+, l_- and l_s) are completely independent from the larger signals from the arm cavity DOFs. This means that the inner DOFs should be capable of staying locked (lengths controlled) while the arm cavities are unlocked (lengths uncontrolled) and randomly passing through carrier resonance.

With the control scheme and interferometer topology described, the control signal for the l_+ DOF should have a DC offset away from the locking point (state in which the DOF is considered to be locked). When modelled using the original model, this DC offset was observed to vary sinusoidally with demodulation phase. When observed using the physical system, no DC offset was apparent. After checking all relevant electronic and optical systems no problems were discovered, which points to a fundamental flaw in the model to physical system conversion.

2 Problems with modelled sidebands

Investigation shows that the modelling tools used to initially develop the sensing scheme (Twiddle and Finesse) do not automatically modulate a modulation. That is to say that if a simulated electro-optic modulator (EOM) is used to put phase sidebands on the model carrier light, and a second modulator is used to impose an additional set of phase sidebands on the carrier light, then the model will not modulate the first set of sidebands. In the physical system, two modulators in series will generate sidebands of sidebands. Therefore we must investigate the effect of these sidebands on the modelled system to find out if the original sensing scheme is still valid using the current physical configuration.

To illustrate this point, the simplest way is to examine the control matrix for the system without sidebands of sidebands (see Table 1) and the same matrix with sidebands of sidebands included (see Table 2). The matrices are very similar with the principal differences being in the response of the signals derived from beat frequencies to the L_+ and L_- DOFs.

	L_+	L_-	l_+	l_-	l_s
$SP : f_1$	1.0000	-0.0000	-0.0012	0.0000	-0.0000
$AP : f_2$	-0.0000	1.0000	0.0000	0.0013	-0.0000
$SP : beat$	-0.0017	-0.0003	1.0000	-0.0320	-0.1127
$AP : beat$	-0.0006	0.0015	0.7441	1.0000	0.0738
$PO : beat$	0.0037	0.0027	0.3318	-0.1760	1.0000

Table 1: *Original normalised control matrix without sidebands of sidebands.*

These changes in the control matrix show that the arm cavity DOFs are not decoupled from the inner DOFs when the sidebands are generated using two phase modulators in series. Therefore, the control matrix representing the current configuration (Table 2) is not valid as a sensing scheme for the 40 m system. The question now becomes; can the current physical system be made to work or must an alternative be found? In order to answer this question it helps to understand how the signals are derived.

	L_+	L_-	l_+	l_-	l_s
$SP : f_1$	1.0000	-0.0000	-0.0012	0.0000	-0.0000
$AP : f_2$	0.0000	1.0000	0.0000	0.0013	-0.0000
$SP : beat$	7.6588	-0.0003	1.0000	-0.0326	-0.1133
$AP : beat$	-0.0006	31.9972	0.7140	1.0000	0.0709
$PO : beat$	3.4554	1.7000	0.1926	-0.0352	1.0000

Table 2: Normalised control matrix with sidebands of sidebands.

3 Signals from double demodulation

A simple picture of the sidebands of sidebands problem can be obtained by examining the equations for phase modulation even before the light interacts with an interferometric system. Phase modulation of light with amplitude E_0 and carrier frequency ω_0 with a modulation of frequency ω_1 and index m gives (to first order)

$$E_1 = E_0 e^{i\omega_0 t} [J_0(m) + iJ_1(m)e^{i\omega_1 t} + iJ_1(m)e^{-i\omega_1 t}]. \quad (1)$$

An identical treatment for a modulation of frequency ω_2 gives

$$E_2 = E_0 e^{i\omega_0 t} [J_0(m) + iJ_1(m)e^{i\omega_2 t} + iJ_1(m)e^{-i\omega_2 t}], \quad (2)$$

and the signal generated if these two modulations are applied in parallel (i.e. the modulators are not in series but are, say, located in separate arms of a Mach Zehnder interferometer) will be given by

$$E_{1+2} = E_0 e^{i\omega_0 t} [J_0(m) + i\frac{J_1(m)}{\sqrt{4}}e^{i\omega_1 t} + i\frac{J_1(m)}{\sqrt{4}}e^{-i\omega_1 t} + i\frac{J_1(m)}{\sqrt{4}}e^{i\omega_2 t} + i\frac{J_1(m)}{\sqrt{4}}e^{-i\omega_2 t}]. \quad (3)$$

This equation is the same as that given by the original model (except for the $\sqrt{4}$ factors which result from the Mach Zehnder topology) and so use of a Mach Zehnder system to generate dual sidebands would be a viable alternative for the physical system, since for this configuration the original control matrix would be valid.

Equation 3 clearly exhibits only phase modulation. On detection on a photodiode ($P_0 = E_0^* E_0$) (without interaction with an interferometer), the signal at the beat frequencies obtained before demodulation is

$$P_{1+2} = P_0 [\dots + \frac{J_1(m)^2}{4} e^{i(\omega_1+\omega_2)t} + \frac{J_1(m)^2}{4} e^{-i(\omega_1+\omega_2)t} + \frac{J_1(m)^2}{4} e^{i(\omega_1-\omega_2)t} + \frac{J_1(m)^2}{4} e^{-i(\omega_1-\omega_2)t} \dots]. \quad (4)$$

This exhibits a small amplitude modulation at the beat frequencies of the sidebands. In the original model, it is this effect which causes the DC offset in the demodulated signals and results only from the beat between sidebands (no effect due to the carrier light). It should be noted that this amplitude modulation is only present once the light is detected on a photodetector and has the same effect as amplitude modulation sidebands of order $J_1(m)^2$. With this in mind we have dubbed the effect as being due to ‘hidden’ sidebands (of sidebands) and, while not strictly true, this serves to distinguish between this effect and the effect of ‘real’ sidebands.

In contrast, the current physical modulation topology (series phase modulators) gives

$$E_{1 \times 2} = E_0 e^{i\omega_0 t} [J_0(m) + iJ_1(m)e^{i\omega_1 t} + iJ_1(m)e^{-i\omega_1 t}] \times [J_0(m) + iJ_1(m)e^{i\omega_2 t} + iJ_1(m)e^{-i\omega_2 t}] \quad (5)$$

$$\begin{aligned} &= E_0 e^{i\omega_0 t} [J_0(m)^2 + iJ_0(m)J_1(m)e^{i\omega_1 t} + iJ_0(m)J_1(m)e^{-i\omega_1 t} \\ &\quad + iJ_0(m)J_1(m)e^{i\omega_2 t} - J_1(m)^2 e^{i(\omega_1+\omega_2)t} - J_1(m)^2 e^{-i(\omega_1-\omega_2)t} \\ &\quad + iJ_0(m)J_1(m)e^{-i\omega_2 t} - J_1(m)^2 e^{i(\omega_1-\omega_2)t} - J_1(m)^2 e^{-i(\omega_1+\omega_2)t}], \end{aligned} \quad (6)$$

which exhibits the same phase modulation sidebands at ω_1 and ω_2 as Equation 3 but also exhibits amplitude modulation sidebands of order $J_1(m)^2$ at the beat frequencies $\omega_1+\omega_2$ and $\omega_1-\omega_2$. Note that these amplitude modulation sidebands are present before detection of the light on a photodetector and will thus be termed ‘real’ sidebands (of sidebands).

On detection of this signal on a photodiode (without interaction with an interferometer), the signal at the beat frequencies obtained before demodulation is

$$\begin{aligned}
P_{1 \times 2} &= P_0[\dots + J_0(m)^2 J_1(m)^2 e^{i(\omega_1 + \omega_2)t} + J_0(m)^2 J_1(m)^2 e^{-i(\omega_1 + \omega_2)t} \\
&\quad + J_0(m)^2 J_1(m)^2 e^{i(\omega_1 + \omega_2)t} + J_0(m)^2 J_1(m)^2 e^{-i(\omega_1 - \omega_2)t} \\
&\quad - J_0(m)^2 J_1(m)^2 e^{i(\omega_1 + \omega_2)t} - J_0(m)^2 J_1(m)^2 e^{-i(\omega_1 - \omega_2)t} \\
&\quad - J_0(m)^2 J_1(m)^2 e^{i(\omega_1 - \omega_2)t} - J_0(m)^2 J_1(m)^2 e^{-i(\omega_1 + \omega_2)t} \dots] \\
&= 0.
\end{aligned} \tag{7}$$

The first four terms in Equation 7 are due to the ‘hidden’ sidebands and the last four terms are due to the ‘real’ sidebands. Note that the terms are all of order $J_1(m)^2$ and cancel each other out on detection by a photodetector. It is due to this effect that the offset expected on the l_+ signal was not present.

The problem is that when an interferometric system is introduced, the ‘real’ sidebands are detected as a beat with the carrier light and so the signal produced by these sidebands on detection are coupled to the arm cavity DOFs. Meanwhile, the ‘hidden’ sidebands are only coupled to the inner DOFs and thus the two sets of sidebands no longer cancel. Hence the large coupling of the L_+ and L_- DOFs into the l_+ , l_- and l_s signals.

4 Demodulation phase

The demodulation phases for the original signals were worked out using the assumption that the arm cavity DOFs were not going to couple into the inner DOF signals. Thus the demodulation phases were optimised for maximum error signal slope for one inner DOF signal with minimum error signal slope for the other two inner DOFs.

This was accomplished by scanning the demodulation phases (once for each modulation frequency) and generating a contour plot showing the relative slopes of all the DOFs at a given photodetector. Simplified versions of these plots are shown in Figures 1, 2 and 3. Each plot shows the full response contour plot of the DOF for which the detector is intended to give the largest signal and the lines of zero response for the other DOFs. The thick, black lines in each plot represents the phases for which the detected error signals have no DC offset at the operating point.

Examination of these plots shows the complexity of the problem. Taking the l_- DOF detected at the AP port as a clear example, the best point for the original control matrix was where the l_+ and l_s lines of zero response cross the zero DC offset line. Some coupling between these signals is acceptable, since the signals from the inner DOFs are all of the same order. By this criteria a reasonable point would be around $phase1 = 180$ and $phase2 = 170$ where the dark blue and green lines cross the black line of zero offset. This point will give a stronger response for l_- than for l_+ and l_s .

However, the problem is immediately clear if one then regards the responses for the L_+ and L_- DOFs. In the AP plot the zero response for the L_+ roughly follows the zero DC offset line and therefore crosses the l_+ and l_s zero response at the same point as used for the original matrix. This feature is made clear by the small AP:beat response to the L_+ DOF in the new control matrix which includes the sidebands of sidebands effect. The zero response for the L_- DOF does not cross the zero DC offset line at the same point and, as can be seen in the control matrix, the L_- response at the AP:beat detector is large in comparison to the l_- response.

Investigation shows that the best pair of demodulation phases to diagonalise the normalised control matrix is given by the point at which the L_+ and L_- zero response lines cross. Using this information, is it possible to generate a diagonalised control matrix for the current physical system simply by careful setting of the demodulation phases?

Yes, but with several reservations. If one examines the PO:beat contour plot, it is obvious that the zero response lines for the L_+ and L_- DOFs never cross. Thus the PO:beat detector cannot be used to detect any of our signals and we must find another monitoring point from which to derive an l_s error signal. In order to make this work, a certain amount of flexibility must be assumed in the selection of demodulation phases.

The most critical factor is that the L_+ and L_- zero response lines do not necessarily cross at the zero DC offset line. In order to sufficiently reduce the L_+ and L_- responses the phases must be within around ± 0.4 degrees of the point at which the zero response lines cross. Thus it was decided to allow selection of points close to, but not necessarily on, the zero DC offset line. In other words, allow the error signals to have DC offsets.

This allows us to choose the point at $phase1 = 146.7$ and $phase2 = 36.0$ on the AP:beat detector to control the

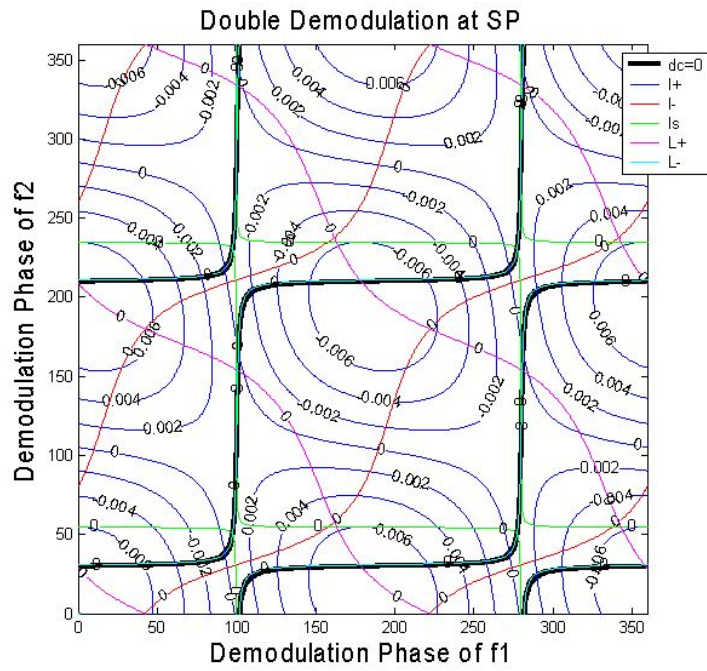


Figure 1: Demodulation phase contour plot for the SP:beat detector.

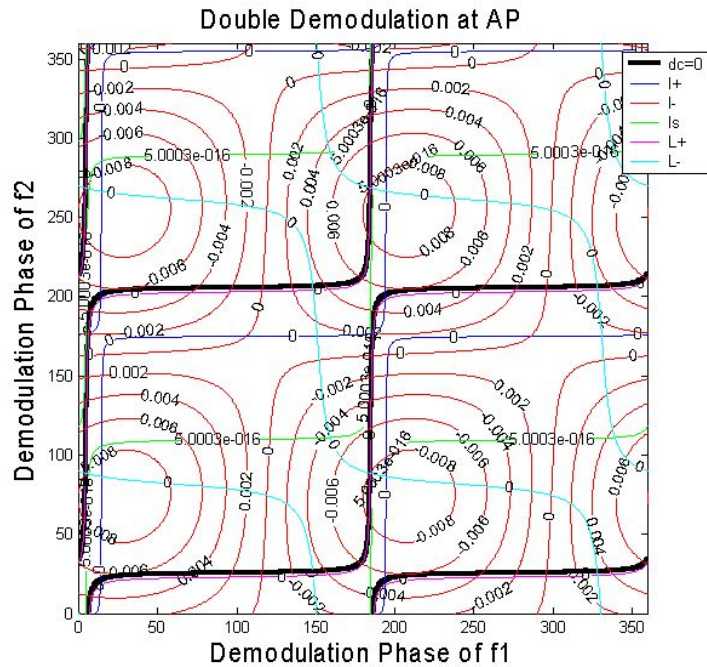


Figure 2: Demodulation phase contour plot for the AP:beat detector.

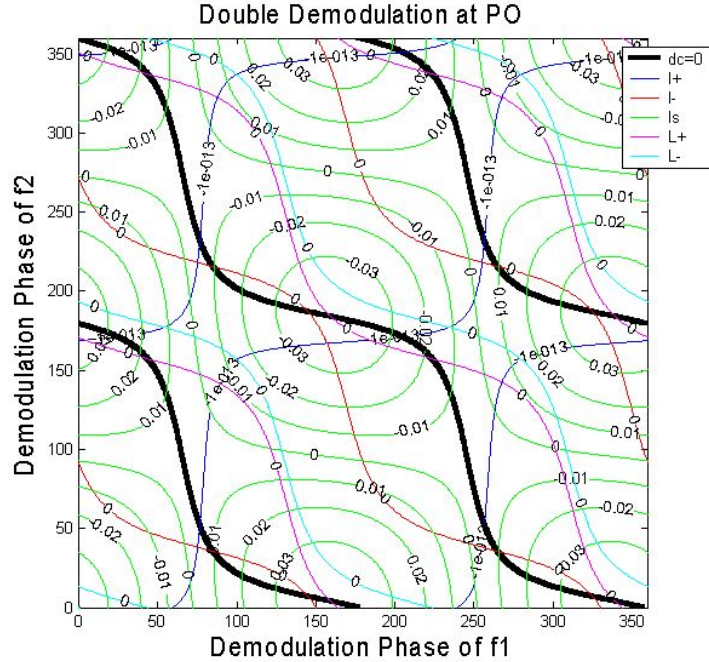


Figure 3: Demodulation phase contour plot for the PO:beat detector.

l_s DOF. The l_+ DOF is still detected on the SP:beat but now with $phase1 = 190.0$ and $phase2 = 18.7$ and the l_- is still detected at the AP:beat detector but with $phase1 = 4.6$ and $phase2 = 88.5$. This gives what would normally be considered a good control matrix as shown in Table 3.

	L_+	L_-	l_+	l_-	l_s
SP : f_1	1.0000	-0.0000	-0.0012	-0.0000	-0.0000
AP : f_2	0.0000	1.0000	0.0000	0.0013	0.0000
SP : beat	-0.0730	-0.0004	1.0000	-0.0290	-0.1553
AP : beat	-0.0007	-0.0168	0.7162	1.0000	0.0520
PO : beat	0.0033	0.0015	0.8036	0.1893	1.0000

Table 3: Normalised control matrix with sidebands of sidebands and fine tuned demodulation phases. Note that the signals in this matrix have DC offsets at the error point.

Unfortunately, there are two main difficulties with this solution. The first is the presence of DC offsets at the operating point as shown in Figure 4. There are many ways in which a DC offset can cause problems in a control scheme. Fluctuations in the light power will couple directly to the signal operating point - as the power changes the offset will change and the mirror will move away from the desired tuning by a fraction of a degree. It is also possible to couple in mirror pointing noise since a slightly misaligned cavity will give changes in the detected power (the required offset will change too).

The second difficulty is that this new demodulation state requires very strict limits on the demodulation phase. If the phases are wrong by ± 0.4 degrees (as mentioned above) the L_+ and L_- DOFs will dominate. This state is almost impossible to achieve since attaining accuracy of this kind would require the whole system to be locked and the offending signals minimised, but the system will not lock until such accuracy is achieved due to the presence of the L_+ and L_- DOF components in the inner DOF sensing signals.

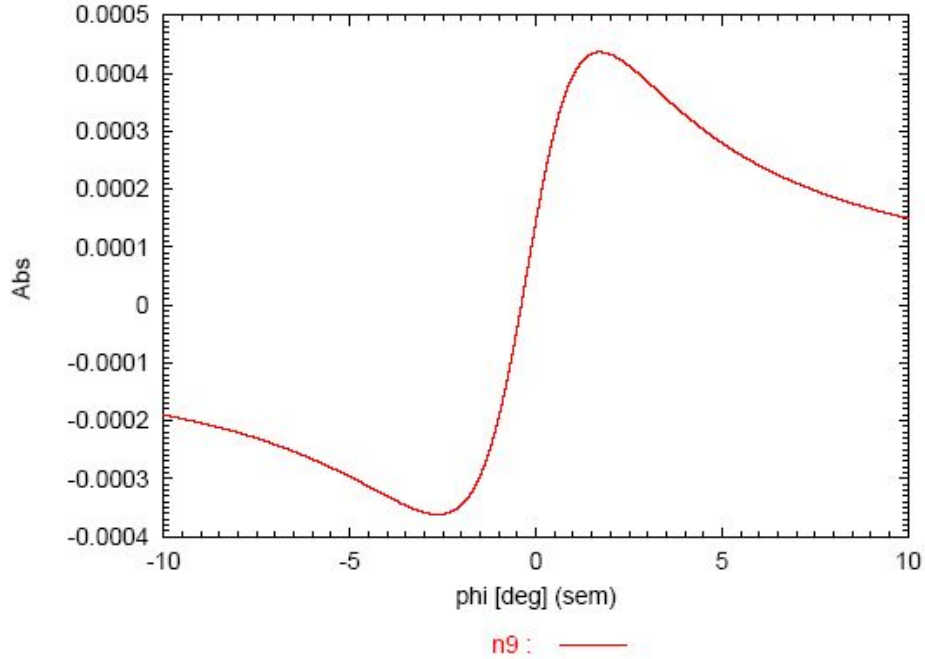


Figure 4: Error signal for the l_s DOF as detected using demodulation phases optimised for low L_+ and L_- sensitivity. Note the presence of a large DC offset at the operating point.

5 Conclusion

It is clear that two phase modulators in series cause significant problems when applied as part of a double demodulation sensing and control scheme for a DRSE interferometric system such as the Caltech 40 m system. It is judged that the difficulties involved in making the system in the current series configuration work (by careful setting of the demodulation phases) would be too difficult to achieve in practice.

The alternative method being considered is the Mach Zehnder option briefly referred to earlier. While this option will reduce the overall sideband power by a factor of four, the use of a Mach Zehnder interferometer will allow the use of all the plans and control methods already considered for the 40 m system.